Attitude determination and monitoring of three-axis controlled satellites with photometric observations

Adrián de Andrés

GMV, Calle Isaac Newton 11, Tres Cantos, 28670, Spain, adandres@gmv.com

Jorge Rubio[1,2], Carlos Paulete[1], Diego Tirado[1], Ángel Gallego[1], Diego Escobar[1], Alfredo M. Antón[1]

[1] GMV, Calle Isaac Newton 11, Tres Cantos, 28670, Spain, jorge.rubio.anton@gmv.com, cpauleteperianez@gmv.com, ditirado@gmv.com, agtorrego@gmv.com, descobar@gmv.com, amanton@gmv.com

[2] Universidad Carlos III de Madrid, Avenida Universidad 30, Leganés 28911, Spain, jorge.r.anton@alumnos.uc3m.es

ABSTRACT

Characterising Resident Space Objects (RSOs) is becoming increasingly important for both civil and military Space Surveillance and Tracking (SST) and Space Domain Awareness (SDA) applications. This study presents a methodology for determining and monitoring the attitude of three-axis controlled satellites with known shape and dimensions through photometric observations, making reasonable assumptions about the materials on the object's surface and their optical reflective properties. The process is based on an Unscented Kalman Filter (UKF), which allows to estimate the satellite's attitude evolution from a reference pointing law, through near real-time sequential processing of the photometric observations. Another algorithm, based on a Least Squares Method (LSM), is also presented and utilised to estimate the satellite's size, using photometric observations and assuming that the shape of the object is known and its attitude follows a nominal pointing law during the observation interval. In both cases, the estimation process relies on comparing real observations with simulated observations obtained from the estimated attitude. Simulated observations are computed using a high-fidelity simulator implemented in OpenGL, which accurately calculates the reflected light contributions from each illuminated surface of the object, accounting for self-shading effects between different components.

The proposed methodology has been thoroughly validated using real photometric observations of a satellite with well-defined shape, size, and attitude, yielding highly promising results. Following this validation, the methodology is used to characterise the Russian Olymp-K-2 satellite —a geostationary communications satellite suspected of signal intelligence (SIGINT) activities— by initially estimating its size based on the approximate shape and nominal pointing law inferred from the limited public data available, and subsequently monitoring its attitude. The monitoring system employs a database to archive the outputs of each determination process and a *Grafana* dashboard to display the results, including thresholds, limits, and alerts, through a user-friendly graphical interface for efficient review and analysis. The results demonstrate the methodology's promising performance in characterising and monitoring the attitude of potentially hostile or unknown satellites through the sequential processing of photometric measurements, offering a responsive and efficient means for near real-time detection of attitude changes.

1. INTRODUCTION

Routine operations in Space Surveillance and Tracking (SST) have traditionally encompassed orbit determination from sensor measurements, such as those obtained from telescopes and radars, for the cataloguing of Resident Space Objects (RSOs). This process facilitates conjunction detection, collision risk estimation, and collision avoidance activities, thereby ensuring the safety, security, and sustainability of space operations. However, in recent years, we have witnessed the dawn of the New Space era, characterised by a proliferation of commercial enterprises, reduced launch costs, and innovative technologies that democratize space utilisation. This paradigm shift signifies that space is no longer the exclusive domain of a few select nations but has become accessible to many stakeholders with diverse economic, scientific, and military interests.

Consequently, outer space has become a strategic domain where merely knowing the orbits of RSOs is insufficient to protect space assets and the space environment from potential threats, traffic congestion and the proliferation of space debris. This evolving requirement has led to the development of Space Domain Awareness (SDA), which extends beyond traditional SST activities to provide a comprehensive understanding of orbital objects from a more holistic perspective. Space object characterisation involves identifying and estimating a range of physical and spectral properties of RSOs, including their size, shape, equipment, materials, rotation, attitude and electronic signatures. This enhanced knowledge is critical for emerging civil activities such as Active Space Debris Removal (ADR) and In-Orbit Servicing (IOS). Additionally, it is of immediate strategic importance in military applications, where detailed insights into other satellites' missions, capabilities, and intentions are essential.

The estimation of an RSO's features from photometric intensity measurements of light reflected from the space object, detected by a ground-based optical sensor, is known as the light-curve inversion problem and presents significant challenges. The primary issue is the intrinsic ambiguity in measurements, where multiple combinations of an RSO's parameters (shape, size, attitude, etc.) can produce equivalent photometric signatures. This work focuses on the estimation of the size and attitude from photometric measurements of potentially hostile RSOs of which there is few public data available. The proposed methodology is validated with real photometric observations of a real satellite with well-known shape, size and attitude, obtaining very accurate results.

Firstly, a Least Squares Method (LSM) is used to estimate the size of an RSO, specifically by determining the scale factor to an assumed shape, while making reasonable assumptions about the object's surface reflective properties and its nominal attitude law, inferred from its mission. The LSM estimates unknown parameters by minimizing the sum of squared deviations between observed data and model predictions. This method is defined by an objective function, which is the residual sum of squares, and it uses linear algebraic techniques to derive parameter estimates. The LSM has been extensively utilized in orbit determination problems [1] and in applications related to object characterisation, such as the estimation of attitude and body parameters [2].

Once an accurate estimate of the RSO's size has been obtained, the attitude can be determined by applying Kalman filtering to estimate the true attitude as a deviation from an assumed attitude law. A Kalman filter is an advanced recursive algorithm employed for estimating the future state of a dynamic system from a series of incomplete and noisy measurements. The filter iteratively predicts the system's state and refines this prediction based on new measurements. This probabilistic approach enables the Kalman filter to deliver an optimal estimate of the system's state in the least-squares sense. There are several types of Kalman filters: the standard (or Linear) Kalman Filter is used for systems modelled with linear functions of the state parameters; the Extended Kalman Filter (EKF) is designed for non-linear systems and approximates non-linear functions by linearizing them around the current state estimate; and the Unscented Kalman Filter (UKF) addresses the limitations of the EKF with a deterministic sampling technique, known as the unscented transform, to accurately capture mean and covariance estimates in highly non-linear systems.

Sequential attitude estimation from photometric measurements has frequently employed UKFs to address the nonlinearity in system dynamics and uncertainty propagation, while avoiding the complexities of partial derivative calculations. Wetterer and Jah [3] demonstrates the application of an UKF for estimating the attitude of a simulated rocket body, modelled as a rotating cylinder, using its light-curve while assuming precise knowledge of its shape and surface reflectance. Their study evaluates the UKF's convergence by varying initial estimates for the attitude, including offsets in Euler angles and angular velocity, within 3-sigma of the true values. The UKF reliably determines the correct attitude parameters across these offsets. However, the study also highlights that when initial attitude offsets are excessively large, the UKF encounters difficulties in converging to the correct solution. This issue arises from the symmetry of the object, which can result in nearly identical light-curves for different rotation-axis positions.

The study by Linares et al. [4] also leverages the UKF to introduce a method for estimating the shape of an RSO, along with its rotational and translational states. Specifically, the approach employs a Multiple-Model Adaptive Estimation (MMAE) technique, which utilises a bank of UKFs, each associated with a different candidate shape model. The state estimate is derived as a weighted sum of the estimates from each filter. The analysis is performed using a simulated space object and a bank of quadrangular prism shape models with known surface reflectance properties. In one scenario, the true model is included within the filter bank, while in another, the true model is represented as a combination of two models from the bank. The results demonstrate effective convergence in estimating the shape and the rotational dynamics in both scenarios, with the attitude determined to within 1 deg of uncertainty and the attitude rate to within 1 deg/h.

Recent research has proposed variants of the UKF to enhance its accuracy in estimating the attitude of an RSO from its light-curve. Rush et al. [5] introduce two UKF formulations: one for cases where the object spins about a constant axis, and another for tumbling scenarios. Both formulations are evaluated using simulated light-curves, with the tumbling formulation also applied to real data. The results highlight the challenges inherent in the light-curve inversion problem, such as the existence of multiple attitude states that produce equivalent light-curves, and the difficulties in validating these methods with real data. Similarly, Cabrera et al. [6] propose the Adaptive Gaussian Mixtures Unscented Kalman Filter (AGMUKF), which models the state probability density function as a Gaussian Mixture to better capture the nonlinearities of the light-curve measurement model. The classical UKF is then applied to each component of the mixture. This approach demonstrates improved convergence robustness, albeit with increased computational complexity due to the merging of the mixture components.

Finally, it is worth mentioning that particle filtering is the current state of the art used in attitude estimation from light-curves [7] [8]. The particle filter is an approximate Bayesian estimator that represents probability densities using a weighted set of samples (particles), enabling effective handling of non-Gaussian probability density functions (PDFs). While the particle filter can address the limitations of the UKF in managing multimodal PDFs resulting from measurement ambiguities and the highly nonlinear measurement function, the UKF is deemed adequate for the specific application described in this work. Here, where a nominal attitude law is assumed and biases relative to it are estimated, the UKF provides accurate results while circumventing the significantly higher computational burden associated with particle filters, which are affected by the curse of dimensionality.

2. METHODOLOGY

2.1 Estimation of size and surface reflective properties using a LSM

Light-curves are influenced by a range of parameters, including the object's orbit, attitude, shape, size, surface reflective properties (encompassing both diffuse and specular reflectance), surface roughness, and atmospheric conditions. In this section, a method for estimating an object's size and reflective properties is introduced. This method presumes that the object's orbit and atmospheric conditions are perfectly known. Additionally, an attitude law must be assumed, and preliminary information regarding at least the proportions between the object's different dimensions is required. With this information, the size can be calibrated by estimating a scale factor for the initial guess of the object's geometry or the optical characteristics of its surfaces. These parameters are often difficult, if not impossible, to ascertain a priori in practical scenarios involving the characterisation of unknown and potentially hostile RSOs.

As previously noted, the surface reflective properties are primarily determined by three parameters: the specular coefficient (K_s), the diffuse coefficient (K_d), and the roughness coefficient (N_s), the latter only involved in specular reflections. Specular reflection impacts photometric measurements only under very specific Sun-satellite-observer geometries, where the satellite-observer direction is symmetrical to the light incidence direction relative to the surface normal. This effect is further constrained when the satellite is modelled with flat surfaces, resulting in a highly narrow reflection beam. Consequently, diffuse reflection emerges as the predominant factor influencing photometric measurements and, therefore, the resulting light-curve used for object characterisation. Accordingly, the subsequent studies are centred on the assessment of diffuse reflection.

Before detailing the method developed, a sensitivity analysis is conducted to evaluate the influence of both the scale factor and the diffuse reflection coefficient on the light-curve. This assessment is intended to demonstrate the interdependence of these parameters, showing that variations in either parameter produce equivalent effects on the light-curve. The analysis utilizes the model of the SMOS (Soil Moisture and Ocean Salinity) satellite, part of the European Space Agency's Earth Explorer missions [9]. The SMOS satellite operates in a sun-synchronous polar orbit with a mean altitude of 758 km. It is equipped with the Microwave Imaging Radiometer with Aperture Synthesis (MIRAS), a passive microwave 2-D interferometric polarimetric radiometer. The SMOS spacecraft features an attitude in which the boresight of the antenna is forward tilted by 32.5º with respect to nadir. This configuration enables measurements at line-of-sight angles between 0 – 50 deg. The satellite employs yaw steering about the local normal. Fig. 1 illustrates the artist's view of the SMOS flight configuration, while Fig. 2 presents the simplified model used for simulating the photometric measurements. As observed, the simplified model retains the major reflecting surfaces of the SMOS satellite —namely, the satellite platform, the solar arrays, and the instrument— preserving the proportional significance of each component.

Fig. 1. SMOS flight configuration [9]

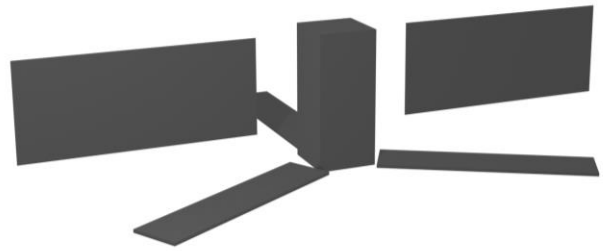

Fig. 2. SMOS simplified model

Regarding the reflective properties of the various components, the solar arrays are modelled as low-reflective, mirror-like surfaces with a diffuse reflection coefficient K_d = 0 and a specular reflection coefficient K_s = 0.1 [10][11]. The unique characteristic of the three antennae facing the Earth is represented with a higher specular reflection coefficient of K_s = 0.7. The roughness coefficient of these surfaces is uniformly set to 0.1, as they are considered flat. The diffuse reflection coefficient for both the platform and the instrument is assumed to be identical. The impact of varying this coefficient, along with the scale factor, on the light-curve is evaluated in the sensitivity analysis presented below.

Before conducting the sensitivity analyses, the results obtained using the simplified model of the SMOS satellite are validated against real photometric observations retrieved from the MMT-9 telescope database [12][13]. The simulated light-curve is generated using this simplified model of the SMOS satellite with a diffuse coefficient of K_d = 0.15, which is a good approach for MLI [11][14][15], and the attitude law described in [9]. The satellite orbit is derived from publicly available Two Line Elements (TLEs) corresponding to the observation times from the MMT-9 telescope, as retrieved from the Space-Track catalogue [16]. The results, presented in Fig. 3, demonstrate a generally good match between the real and simulated light-curves. While the simplified model omits finer details, leading to the loss of some oscillatory behaviour present in the actual light curve, the overall correspondence remains satisfactory.

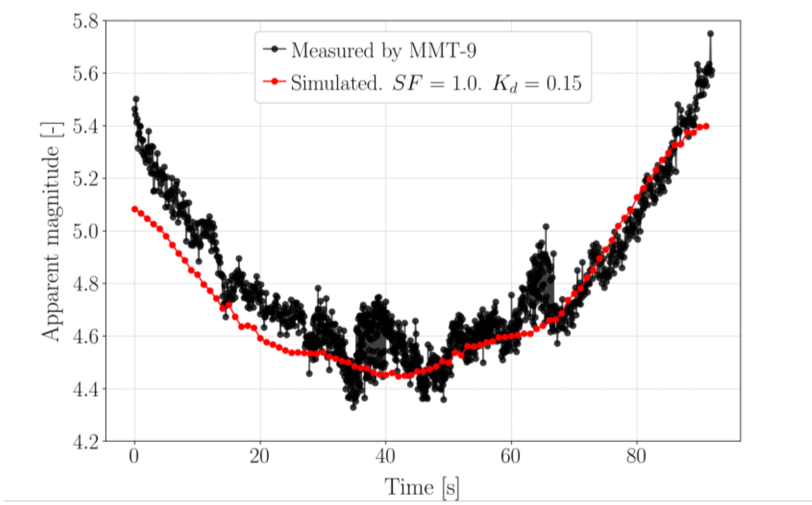

Fig. 3. Comparison of real and simulated light-curves for the SMOS satellite

The results of the sensitivity analysis on the scale factor are shown in Fig. 4 for a constant diffuse coefficient of 0.15, while the results of the sensitivity analysis on the diffuse coefficient are shown in Fig. 5 for a constant scale factor of 1.0. These results show the equivalence in the effect of these two parameters on the light-curve, thereby demonstrating the impossibility of estimating them simultaneously.

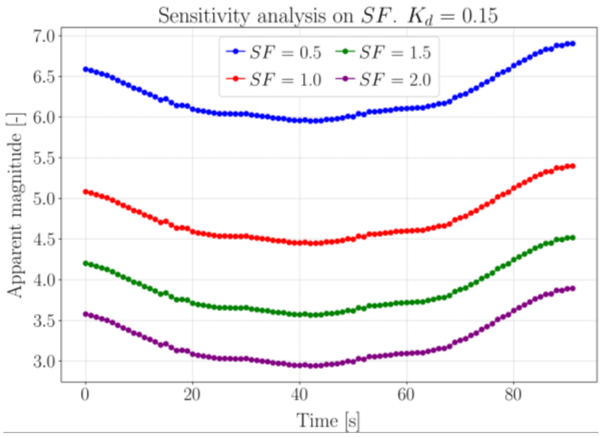

Fig. 4. Sensitivity analysis on the scale factor

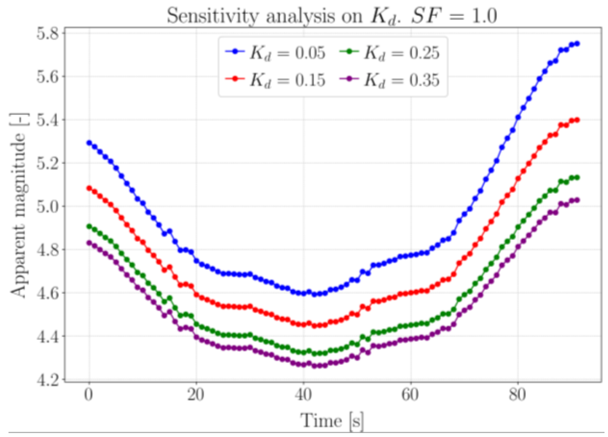

Fig. 5. Sensitivity analysis on the diffuse coefficient

Given that the scale factor and the diffuse coefficient induce an upward or downward shift in the magnitude of the photometric observations, these parameters can be estimated using a LSM. This method, which is designed to iteratively locate the solution in the proximity of a specified initial guess, retaining the solution that minimises the discrepancy between simulated and actual measurements. During each iteration, the filter calculates the root mean square (RMS) of the deviations between the actual photometric measurements and the simulated values, employing the current estimate of the parameter (scale factor or diffuse coefficient). It then proposes a new parameter value based on these discrepancies and the partial derivatives of the measurements with respect to the parameter being estimated. Convergence is achieved when the relative change in RMS between successive iterations is less than 0.1%.

Therefore, resolving the light-curve inversion problem requires a high-fidelity simulator of photometric observations. In this work, GMV's ***Grial*** tool is used, an advanced high-fidelity simulator implemented in OpenGL that calculates the contribution to the reflected light from each illuminated and visible pixel on a 3D shape and adds their contributions. It employs the Cook and Torrance BRDF [17] for the specular reflection, but with the Beckmann's distribution proposed there replaced by the one proposed by Walter in the GGX model [18], and the Lommel-Seeliger BRDF [19] for the diffuse reflection. The advantages of these BRDF being the fact that they are based in the actual optical properties of the materials on the surface of the object and proved to be very realistic.

Revisiting the results from the sensitivity analyses presented earlier, it is evident that simultaneous estimation of both parameters is unfeasible due to their variations producing equivalent effects on the resultant light-curve. Consequently, this study concentrates on calibrating the shape of the space object, specifically by estimating the scale factor, while making reasonable assumptions regarding the diffuse reflection coefficient for the various surfaces of the object model.

2.2 Attitude estimation using an UKF

Once the size and optical properties of the space object have been accurately determined, its attitude can be estimated relative to a predefined pointing law, which acts as a baseline or initial guess. The focus of this analysis is on three-axis stabilized satellites. To effectively solve this light-curve inversion problem, an UKF is employed, offering both accurate results and robust computational performance. The UKF iteratively refines the predefined attitude law by processing photometric measurements, making precise adjustments to the attitude estimate to enhance the alignment between simulated and observed light-curves. The root mean square (RMS) error is utilized to quantify the standard deviation of the differences between predicted and observed values, thereby assessing the accuracy of the estimation.

In the UKF, the estimation process starts by predicting the state and its associated uncertainty at the subsequent time step using a set of sigma points. These sigma points are strategically selected to represent the distribution of the state around the estimated mean, aiming to approximate the true distribution after nonlinear transformations. The UKF propagates these sigma points through the nonlinear dynamic model, thereby enhancing the filter's accuracy in managing non-Gaussian and highly nonlinear systems. Subsequently, the predicted state is used to estimate the expected measurements. The Kalman gain is then computed to determine the degree of correction needed for the predicted state based on the deviation between predicted and actual measurements. This gain is crucial for adjusting the predicted state in each iteration, allowing the UKF to incorporate new measurements and refine the system state estimation continuously. By iteratively updating the state with the Kalman gain, the UKF enhances accuracy and reduces uncertainty. In this study, the implementation of the UKF from the *Hipparcus* library [20] is utilized.

Before further discussing the methodology, preliminary analyses have been conducted to highlight the challenges of attitude estimation from light-curves and to demonstrate the advantages of using an UKF to address them. These studies also utilize the SMOS satellite model presented in Section 2.1, and the optical parameters previously retained for the three main components of this satellite (the platform, the three antennae facing the Earth and the solar arrays), to showcase the UKF's potential capabilities.

The first study aims to validate the accuracy of the UKF in estimating the attitude of three-axis stabilized satellites through a statistical evaluation. This assessment involves analysing 50 different light-curves, each resulting from a distinct inertial pointing law. For each light-curve, the true attitude is estimated using the UKF, which is initialized with varying Initial Orientation Errors (IOEs). These IOEs are generated by rotating the initial orientation around a randomly selected axis relative to the true inertial attitude. The results are visualized using a box plot, which presents the mean angular error and RMS error for different IOE values, highlighting the median, quartiles, and whiskers.

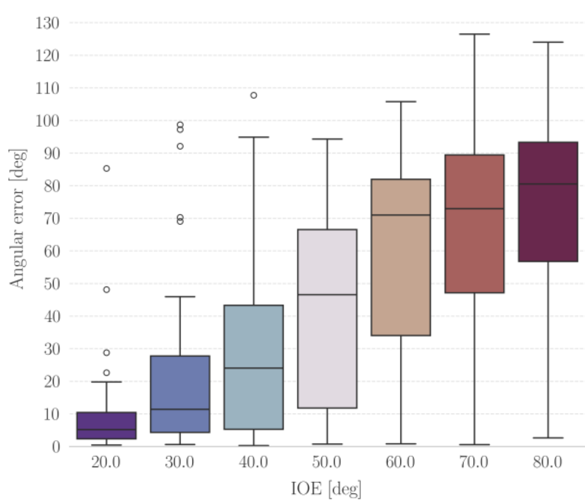

Fig. 6. Angular error results of statistical analysis

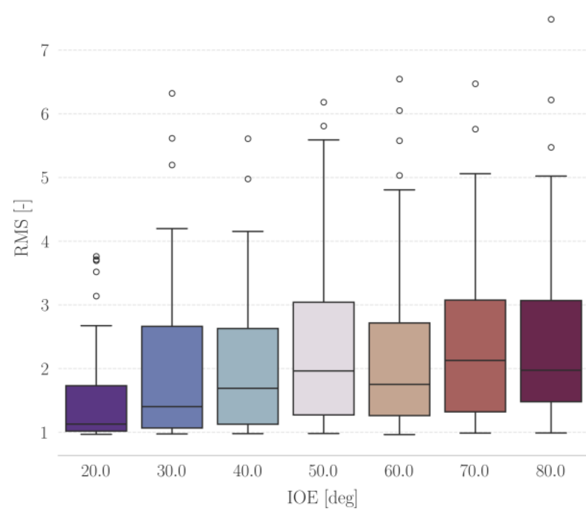

Fig. 7. RMS results of statistical analysis

As illustrated in Fig. 6, an increase in IOE correlates with a corresponding rise in the mean angular error, highlighting the stringent requirement for an accurate initial guess for the UKF to converge to the true attitude. When considering operationally feasible IOEs, the data reveals that the median mean error for IOEs of 20 degrees and 30 degrees is approximately 5 degrees and 12 degrees, respectively. These finding demonstrate the UKF's promising feasibility for solving the light-curve inversion problem in attitude estimation. Conversely, Fig. 7 indicates that the RMS does not increase as consistently as the mean angular error with rising IOE, with median RMS values generally ranging between 1 and 2. This result indicates the presence of numerous favourable local minima in the light-curve inversion problem, confirming that different attitude laws can produce identical photometric measurements.

Another pertinent analysis centres on the shape model of the space object employed in the simulation of photometric observations. Specifically, the effects of variations in the model on the resulting simulated light-curve are assessed using the SMOS satellite. As previously mentioned, the SMOS satellite comprises three main components: the platform, the solar arrays, and the three antennae facing the Earth (instrument). Various combinations of these elements are tested to ascertain their individual contributions to the light-curve.

The statistical analysis follows the same methodology as the previous evaluation of the UKF's estimation accuracy as a function of the IOE, utilising 50 light-curve analyses, each corresponding to a distinct inertial attitude law. A set of variable IOEs, ranging from 10 degrees to 60 degrees, has been employed. In this analysis, the results are presented in a line plot, with each line representing a model composed of different elements of the SMOS satellite: only the platform, the platform with the solar array, the platform with the instrument, and the platform with both the solar array and the instrument. Both the angular error relative to the true attitude and the RMS relative to the true photometric measurements are presented in Fig. 8 and Fig. 9, respectively.

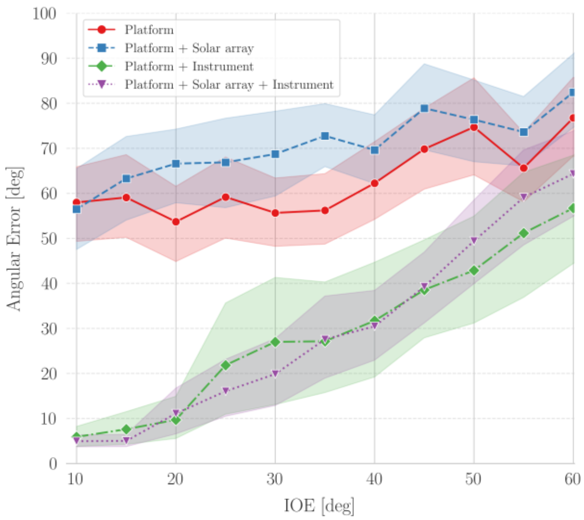

Fig. 8. Angular error results for different RSO models

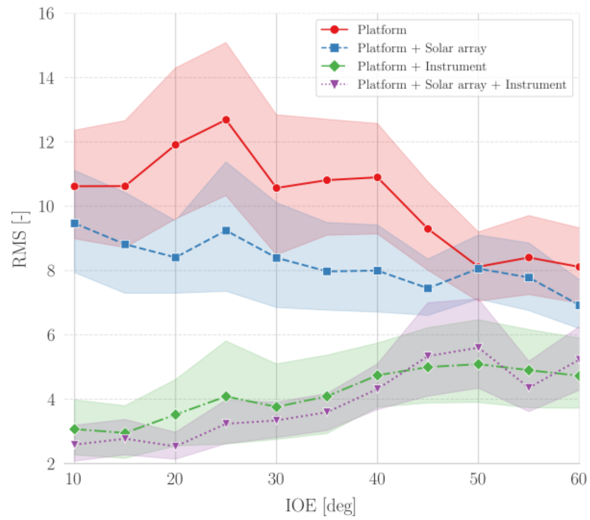

Fig. 9. RMS results for different RSO models

The most evident conclusion from the results is that both the complete model (including all components) and the model excluding only the solar arrays exhibit the best accuracy in terms of absolute angular error and RMS. Conversely, the estimations using models that exclude the instrument (whether with or without the solar arrays) show significant deviations from the true attitude law. This highlights the critical impact of the instrument's reflected light on the resulting light-curve. Notably, the model without the solar arrays performs better than the model without the instrument, likely due to potential self-shadowing effects of the solar arrays under certain inertial attitude laws. These self-shadowing effects can lead to less precise observations and inaccurate final attitude estimations due to the obstruction of key elements in the observations. This result is expected for a satellite in LEO, but for satellites in GEO, the solar arrays are crucial for accurately estimating the light curve due to their larger size and the nearly constant observer-satellite geometry. Regarding the convergence of the UKF to the true attitude state, the results align closely with those presented in Fig. 6 and Fig. 7, showing promising convergence properties for IOEs below 30 degrees.

Finally, for demonstration purposes, the real attitude of the SMOS satellite is estimated using the UKF, with the initial estimate assuming a Nadir-pointing attitude law. Fig. 10 shows the light-curve generated by the attitude law to which the UKF converges in its final iteration. For comparison, the results previously shown in Fig. 3 are also included. The UKF converges to a solution close to the actual attitude of the SMOS satellite, achieving a better match with the actual light-curve measured by the MMT-9 telescope during the initial phase, though it shows a slight deviation in the latter part. The angular error with respect to the true attitude is 3.5 degrees, and the resultant RMS error is similar to that obtained for the simulated light-curve using the actual attitude, being similar to the noise of the measurements (~0.1). These results demonstrate the challenges in solving the light-curve inversion problem for attitude estimation, primarily due to the inherent ambiguities in the measurements and the limited knowledge of the RSO's geometrical and optical properties.

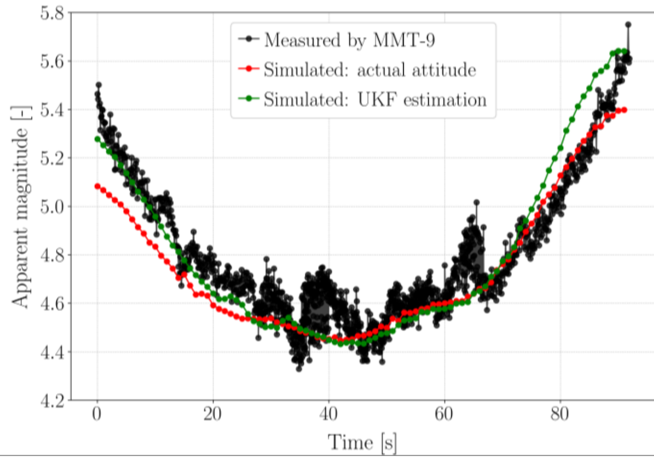

Fig. 10. UKF-estimated light-curve for the SMOS satellite

3. RESULTS

Once the proposed methodology has been validated and the promising performance of both the LSM filter for size estimation and the UKF for attitude estimation of three-axis stabilized satellites has been demonstrated, this section focuses on the analysis of suspected signal intelligence (SIGINT) satellites in geostationary orbit, specifically the Russian Olymp-K-2 satellite, also designated Luch-Kh. The analysis uses the limited public data available regarding their potential shape, dimensions, and attitude law as a reference.

3.1 Estimation of size and surface reflective properties using a LSM

The study begins with an accurate estimation of the satellite's shape, size, and optical properties. This is accomplished by making reasonable assumptions regarding the shape and reflective characteristics of the satellite's surfaces, and employing the LSM to estimate a scale factor that aligns the real and simulated photometric measurements. This approach builds on the preliminary analyses presented in Section 2.1, which demonstrated that estimating both the size and the reflective properties simultaneously is not feasible. Consequently, reasonable assumptions about the object's shape and, particularly, the reflective properties of the satellite's surfaces are crucial for accurately estimating the scale factor using the LSM.

Olymp-K satellites are built on ISS Reshetnev's Ekspress-1000NTA bus, with a launch mass of approximately 3000 kg [21]. Detailed geometrical characteristics of the Olymp-K-2 satellite are not publicly available. However, it is assumed to have a shape similar to other geostationary communications satellites of the Luch series [22] [23], such as the Luch-5 satellite depicted in Fig. 11. Based on this mass and assumed shape, an initial estimate of the satellite's dimensions (3x3x5 m for the platform and 3x18 m for the solar arrays) can be inferred from the information provided in the DISCOS database [24] for comparable satellites, such as those in Eutelsat's network with a similar mass. The simplified model used as initial guess is depicted in Fig. 12 below. Dish antennae are not considered due to the difficulty of modelling them without knowing their actual dimensions and orientation. In addition, they are apparently translucent, and such materials cannot be accurately modelled in our light-curve simulator.

Fig. 11. Recreation of the Luch-5 satellite [21]**¡Error! No se encuentra el origen de la referencia.**

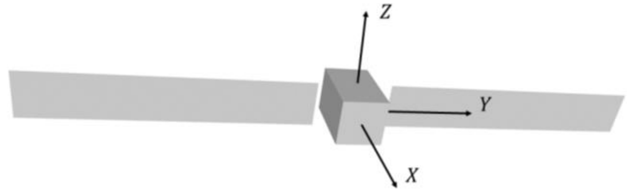

Fig. 12. Olymp-K-2 simplified model

As explained in Section 2.1, estimating the scale factor to match the simulated photometric observations with the real light-curve requires reasonable assumptions about the reflective properties of the satellite's surfaces. According to Qiao et al. [25], who examined the reflectance spectra of six GEO satellites over a ten-month period, the primary factor influencing the reflectance spectra is the Multi-layer Insulation (MLI) on the surfaces of three-axis stabilized GEO satellites. Consequently, the reflective properties applied to the platform of the satellite are those specified for the MLI in Section 2.1. The reflective properties for the solar arrays are also detailed in Section 2.1.

Finally, the LSM filter is applied to estimate the scale factor and adjust the assumed size based on information available for similar satellites. Given that Olymp-K-2 is a data-relay geostationary satellite, a reasonable assumption for the estimation of the scale factor involves a Nadir pointing attitude law, with the X-axis pointing towards the Nadir, the Y-axis normal to the orbital plane, and the Z-axis in the along-track direction of the satellite. The solar arrays are adjusted continuously to maintain optimal alignment with the Sun. The scale factor that minimizes the squared residuals is found to be 1.2.

Figure 12 compares the real light-curve with the simulated photometric measurements, using the previously estimated scale factor of 1.2. Two notable observations emerge from this figure. Firstly, while there is generally a good alignment between the simulated and actual light-curves, a notable discrepancy is observed between 14000 and 26000 seconds, where the simulated model appears to reflect more light than the actual satellite. This discrepancy likely stems from the two antennae on the real satellite, as shown in Fig. 11, which are not accounted for in the simplified model. These antennae, constructed from translucent materials, could block a substantial amount of the sunlight or the light reflected by other components of the satellite. Secondly, the simulated light-curve exhibits a discontinuous behaviour between consecutive data points. This phenomenon has been meticulously analysed and is attributed to the specular reflections from the solar arrays, which fluctuate markedly with variations in both the light incidence angle and the relative position between the sensor and the satellite.

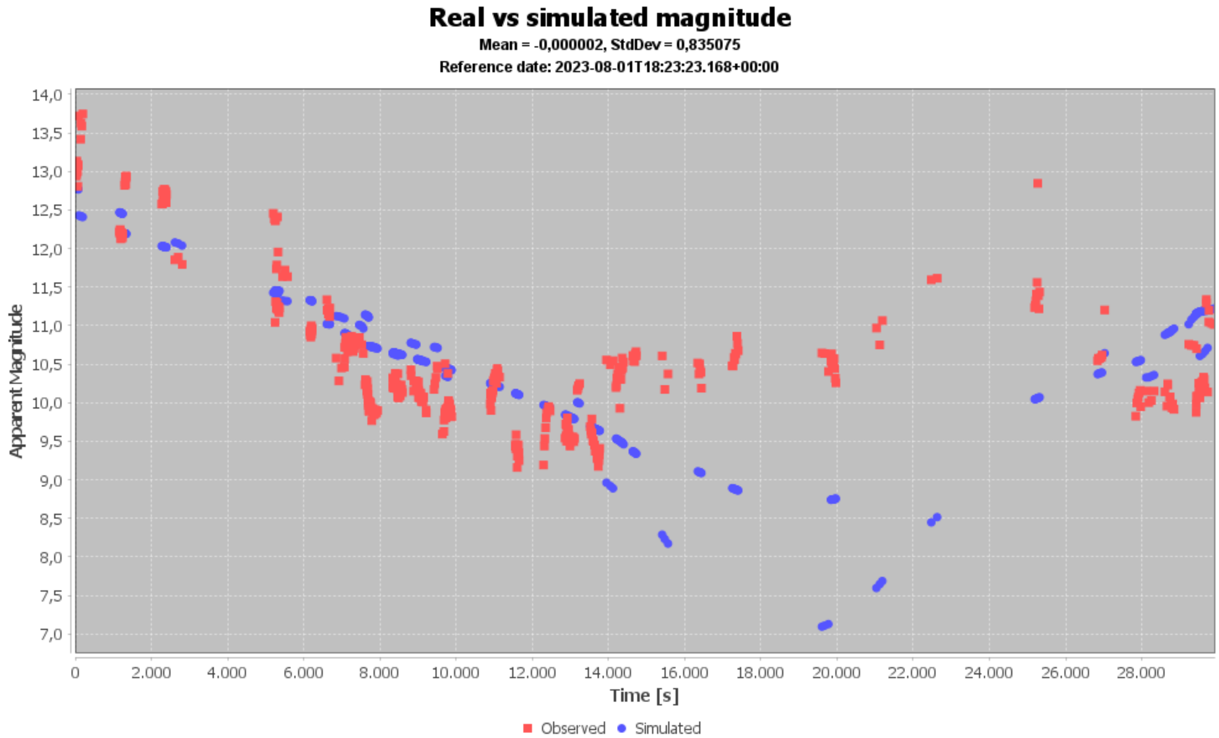

Fig. 13. Comparison of real and simulated light-curves for a scale factor of 1.2

3.2 Attitude estimation and monitoring using an UKF

Finally, once the shape, size, and reflective properties of the Olymp-K-2 satellite have been estimated, the UKF can be used to estimate the attitude and monitor its evolution in near-real time. To achieve this, photometric measurements are processed every 30 minutes, with the attitude estimated for each batch of measurements. In the first iteration, the initial estimate is based on an assumed attitude law inferred from the satellite's mission. In subsequent iterations, the final attitude estimate from the previous iteration is used as the initial estimate for the current iteration.

The monitoring system employs a database to archive the outputs of each determination process and uses a *Grafana* dashboard, such as the one shown in Fig. 14, to display the results, including thresholds, limits, and alerts, thereby providing a user-friendly graphical interface for efficient review and analysis.

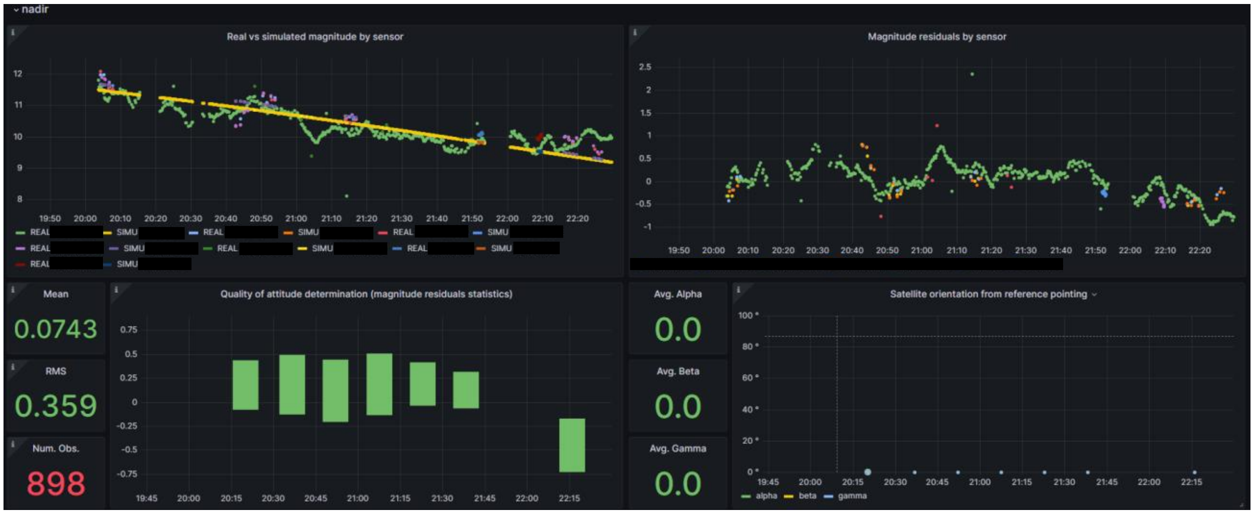

Fig. 14. *Grafana* dashboard for near real-time attitude monitoring

4. CONCLUSIONS

This work presents a novel methodology for characterizing the size and attitude of three-axis controlled satellites with limited public information, using photometric observations. The strategy involves a two-step process: first, the size (as a scale factor to an assumed shape) is estimated using a Least Squares Method (LSM) under reasonable assumptions about the reflectance properties of the satellite's surfaces and its attitude. The initial attitude assumption is based on the satellite's mission and can be refined using an Unscented Kalman Filter (UKF), which adjusts the attitude estimate to improve the alignment between simulated and observed light curves. The methodology has been thoroughly validated with real photometric observations of the SMOS satellite, which has well-defined shape, size and attitude. Following this validation, the methodology is applied to characterise the Russian Olymp-K-2 satellite, a geostationary communications satellite suspected of signal intelligence (SIGINT) activities.

The results of the preliminary analyses of the SMOS, which validated the methodology, as well as the characterization of the Olymp-K-2 satellite, show the challenges of the light-curve inversion problem, primarily due to the inherent ambiguities in measurements and limited knowledge of the satellite's geometrical and optical properties. However, these results also demonstrate the methodology's promising performance in characterising and monitoring the attitude of potentially hostile or unknown satellites through the sequential processing of photometric measurements, even with very limited publicly available information about their physical, optical and orbital characteristics. The monitoring system built on this methodology provides a responsive and efficient means for near real-time detection of attitude changes and features a user-friendly graphical interface that facilitates the analysis of attitude evolution.

ACKNOWLEDGEMENTS

The authors gratefully acknowledge the team of the Mini-MegaTORTORA (MMT-9) system, which belongs to Kazan Federal University, for providing the publicly accessible database of light-curves. The authors also express their appreciation to the European Space Agency for their diligent efforts in maintaining and developing the DISCOS database and its API. Additionally, the authors thank the U.S. Strategic Command for making the catalogue of TLEs publicly available through Space-Track.

REFERENCES

[1] B. D. Tapley, B. E. Schutz, and G. H. Born, *Statistical Orbit Determination*. Elsevier Academic Press, 2004.

[2] D. Hall, B. Calef, K. Knox, M. Bolden, and P. Kervin, “Separating attitude and shape effects for non-resolved objects” in *The 2007 AMOS Technical Conference Proceedings*, Kihei, Maui, HI, Sep. 2007, pp. 464-475, Maui Economic Development Board, Inc.

[3] C. J. Wetterer and M. Jah, “Attitude determination from light curves”, *Journal of Guidance, Control, and Dynamics*, vol. 32, no. 5, pp. 1648-1651, 2009.

[4] R. Linares, J. Crassidis, M. Jah, and H. Kim, “Astrometric and photometric data fusion for resident space object orbit, attitude, and shape determination via multiple-model adaptive estimation” in *AIAA Guidance, Navigation, and Control Conference*, Aug. 2010, p. 8341.

[5] K. Rush, M. Yost, L. Smith, and A. Zizzi, “An application of the unscented Kalman filter for spacecraft attitude estimation on real and simulated light curve data” in *Proceedings of the Advanced Maui Optical and Space Surveillance Technologies Conference (AMOS)*, Maui, HI, USA, 2020.

[6] D. V. Cabrera, J. Utzmann, and R. Förstner, “The adaptive Gaussian mixtures unscented Kalman filter for attitude determination using light curves”, *Advances in Space Research*, vol. 71, no. 6, pp. 2609-2628, 2023.

[7] R. Linares, J. L. Crassidis, and M. K. Jah, “Particle filtering light curve based attitude estimation for non-resolved space objects” in *AAS/AIAA Space Flight Mechanics Meeting*, Jan. 2014, pp. 14-210.

[8] Y. Wang, X. Du, R. Gou, Z. Liu, and H. Chen, “A secondary particle filter photometric data inversion method of space object characteristics”, *Electronics*, vol. 12, no. 9, p. 2044, 2023.

[9] “SMOS (Soil Moisture and Ocean Salinity) Mission”, *EO Portal*. [Online]. Available: https://www.eoportal.org/satellite-missions/smos. [Accessed: Jul. 10, 2024].

[10] Y. Cao, Z. Wu, L. Bai, and H. Zhang, “Measurement of optical characteristics of solar panels used on satellite” in *Proceedings of the 9th International Symposium on Antennas, Propagation and EM Theory*, Guangzhou, China, 2010, pp. 746-748.

[11] H. M. Cowardin, J. M. Hostetler, J. I. Murray, J. A. Reyes, and C. L. Cruz, “Optical characterization of DebriSat fragments in support of orbital debris environmental models”, *Journal of the Astronautical Sciences*, vol. 68, no. 4, pp. 1186-1205, 2021.

[12] S. Karpov et al., “Massive photometry of low-altitude artificial satellites on Mini-Mega-TORTORA”, *Revista Mexicana de Astronomía y Astrofísica (Serie de Conferencias)*, vol. 48, pp. 112-113, 2016.

[13] G. M. Beskin et al., “Wide-field optical monitoring with Mini-MegaTORTORA (MMT-9) multichannel high temporal resolution telescope”, *Astrophysical Bulletin*, vol. 72, no. 1, pp. 81-92, 2017.

[14] M. J. Mirtich and J. S. Sovey, “Optical and electrical properties of ion beam textured Kapton and Teflon” in *National Vacuum Symposium*, Jan. 1977, NASA-TM-73778.

[15] D. P. Engelhart et al., “Space weathering experiments on spacecraft materials”, *The Journal of the Astronautical Sciences*, vol. 66, no. 2, pp. 210-223, 2019.

[16] U.S. Strategic Command, *Space-Track.org*. [Online]. Available: https://www.space-track.org. [Accessed: Mar. 12, 2024].

[17] R. L. Cook and K. E. Torrance, “A reflectance model for computer graphics”, *ACM Transactions on Graphics (ToG)*, vol. 1, no. 1, pp. 7-24, 1982.

[18] B. Walter, S. R. Marschner, H. Li, and K. E. Torrance, “Microfacet models for refraction through rough surfaces” in *Proceedings of the 18th Eurographics Conference on Rendering Techniques*, Jun. 2007, pp. 195-206.

[19] M. B. Fairbairn, “Planetary photometry: The Lommel-Seeliger law,” *Journal of the Royal Astronomical Society of Canada*, vol. 99, no. 3, pp. 92-99, 2005.

[20] “Hipparchus 2.3 API”, *Hipparchus* [Online]. Available: https://hipparchus.org/apidocs-2.3/org/hipparchus/filtering/kalman/unscented/UnscentedKalmanFilter.html. [Accessed: Mar. 26, 2024].

[21] G. D. Krebs, “Luch-Kh/Olimp-K”, *Gunter's Space Page*. [Online]. Available: https://space.skyrocket.de/doc_sdat/olimp-k.htm. [Accessed: Jul. 17, 2024].

[22] A. Zak, “Luch data-relay satellite”, *RussianSpaceWeb.com*. [Online]. Available: https://www.russianspaceweb.com/luch.html. [Accessed: Jul. 17, 2024].

[23] A. Zak, “Luch-5 data-relay satellite series”, *RussianSpaceWeb.com*. [Online]. Available: https://www.russianspaceweb.com/luch5a.html. [Accessed: Jul. 17, 2024].

[24] European Space Agency, “DISCOSweb”, *Space Debris User Portal*. [Online]. Available: https://discosweb.esoc.esa.int. [Accessed: Jul. 20, 2024].

[25] Q. Qiao, Y. Ping, J. Chen, Y. Lu, and C. Zhang, “Investigation of factors affecting the reflectance spectra of GEO satellites”, *Advances in Space Research*, 2024.